

Dipolar and nondipolar interactions in LiTbF_4

L. M. Holmes*

Laboratorium für Festkörperphysik, Eidgenössische Technische Hochschule, CH-8049 Zürich, Switzerland

J. Als-Nielsen

AEC Research Establishment Risø, DK-4000 Roskilde, Denmark

H. J. Guggenheim

Bell Laboratories, Murray Hill, New Jersey 07974

(Received 16 December 1974)

The magnetic interactions in LiTbF_4 have been studied in measurements of the quasielastic scattering of neutrons from the paramagnetic crystal. Scattering data have been collected at a temperature $T = 18.6$ K, which is 6.5 times the Curie temperature of LiTbF_4 , and have been least-squares fitted with an expression for the scattering cross section which includes, in addition to the dominant dipolar coupling, two exchange parameters J_1 and J_2 describing the nondipolar coupling between nearest- and next-nearest-neighbor Tb^{3+} ions, respectively. The derived exchange parameters are $J_1/k = -0.26 \pm 0.09$ K and $J_2/k = +0.05 \pm 0.10$ K. Based on these parameters the total interaction energy for nearest-neighbor ions is $4/3$ dipolar and $-1/3$ nondipolar, and the nondipolar interactions are less important for second neighbors. The interaction Hamiltonian is discussed, the wave-vector-dependent susceptibility $\chi_T(\vec{Q})$ is derived in the mean-field approximation, and the dipolar interactions are evaluated numerically using Ewald's technique.

I. INTRODUCTION

Recent work has shown LiTbF_4 to be an interesting example of a low-temperature Ising-like ferromagnet.^{1,2} The Curie point $T_C = 2.86$ K is easily accessible in pumped liquid helium, the crystal structure is fairly simple (body-centered tetragonal), and the material may be prepared as large, reasonably perfect single crystals. Especially interesting is the fact that magnetic dipolar interactions are strong. LiTbF_4 is a model system for studying dipolar effects in magnetic ordering.

The purpose of this paper is, in essence, to critically examine and test the validity of the last statement. We shall be concerned in particular with the form and magnitude of the magnetic interactions in LiTbF_4 . The experimental technique used is (quasielastic) neutron scattering. The neutron data at a high temperature ($T = 18.6$ K) are compared to a theoretical expression based on the wave-vector-dependent susceptibility $\chi_T(\vec{Q})$, and the nondipolar, or "exchange," contributions to the near-neighbor interactions are thereby quantitatively evaluated. The theoretical (mean-field) expression for $\chi_T(\vec{Q})$ is also derived in this paper, and the dipolar interactions are evaluated numerically.

An initial report on portions of this work has appeared previously.³ That report presented both the wave-vector (\vec{Q}) dependence of $\chi_T(\vec{Q})$ at $T = 38.8$ K and the temperature (T) dependence of

the limiting $\vec{Q} \rightarrow 0$ susceptibility. A long-wavelength ($\vec{Q} \approx 0$) singularity in $\chi_T(\vec{Q})$ was reported and ascribed, in a quantitative comparison with theory, to the magnetic dipolar coupling. In the present paper, the theory is given in considerably more detail. Also, the wave-vector dependence of the susceptibility has been remeasured isothermally at a lower temperature and over a broader range of \vec{Q} values, in order to improve the sensitivity of the data to the form and magnitude of the magnetic interactions. In the following paper⁴ the crystal structure is investigated and measurements of the spontaneous magnetization are presented for temperatures $T > T_C$ and, particularly, in the critical region $T \approx T_C$. A detailed description of the critical behavior of $\chi_T(\vec{Q} \rightarrow 0)$ is planned for a future publication.⁵

II. THEORY

For comparison with the neutron experiment we shall be interested in the wave-vector-dependent magnetic susceptibility $\tilde{\chi}_T(\vec{Q})$ in the paramagnetic state. This quantity describes the response of the crystal (at temperature T) to an applied magnetic field $\vec{H}(\vec{r})$ which is independent of time but which varies spatially through the lattice.⁶ The spatial variation is characterized by the wave vector \vec{Q} , e.g.,

$$\vec{H}(\vec{r}) = \vec{H}(0) \cos \vec{Q} \cdot \vec{r}, \quad (1)$$

where \vec{r} is an arbitrary position. $\vec{H}(\vec{r})$ induces a

magnetization $\vec{M}(\vec{r})$ which varies with the field wave vector \vec{Q} in the crystal, and the amplitude of the magnetization wave is defined as $\bar{\chi}_T(\vec{Q})\vec{H}(0)$. Expressed more formally,

$$\vec{M}_{\vec{Q}} = \bar{\chi}_T(\vec{Q})\vec{H}_{\vec{Q}}, \quad (2)$$

where $\vec{M}_{\vec{Q}}$ and $\vec{H}_{\vec{Q}}$ denote the amplitudes of the \vec{Q} th harmonics of $\vec{M}(\vec{r})$ and $\vec{H}(\vec{r})$, respectively.

The susceptibility is a tensor quantity, but we shall consider only the longitudinal component $\chi_T^{zz}(\vec{Q})$. Only this component is relevant in LiTbF_4 , because the material is Ising-like at low temperatures and can be magnetized only along the c direction.^{1,2} (The coordinates x , y , and z are taken along the tetragonal crystal axes a , a , and c , respectively.) We shall therefore drop the tensor notation in much of the following and identify the scalar $\chi_T(\vec{Q})$ with the longitudinal susceptibility. This quantity describes the response of the crystal to a magnetic field along the spin axis. Of course the wave vector \vec{Q} may take on arbitrary magnitudes and directions.

It is extremely difficult to evaluate $\chi_T(\vec{Q})$ theoretically, even for a relatively "simple" magnet such as LiTbF_4 . One has generally to rely on certain limiting approximations in making connection with experiment. For example the critical behavior is described in the long-wavelength ($\vec{Q} \approx 0$) approximation at small values of the reduced temperature ($t = 1 - T_c/T$), and the high-temperature behavior is described in the "random-phase approximation" at high values of t . The latter approximation will concern us here. It gives a formula which is "asymptotically exact"⁷ as $t \rightarrow 1$. Fortunately, we were able to obtain data in LiTbF_4 at $t = 0.85$, at which temperature the theoretical approximation should be expected to be quite good.

The purpose of this section is to present the theoretical expressions and numerical results pertaining to $\chi_T(\vec{Q})$ which are necessary for interpreting the neutron experiments. The interaction Hamiltonian will be discussed, the high-temperature expression for $\chi_T(\vec{Q})$ will be derived, and the magnetic dipolar interactions will be evaluated numerically. The long-wavelength singularity in $\chi_T(\vec{Q})$ will be considered. Finally, the effects of superexchange coupling will be incorporated in the theoretical expressions.

A. Hamiltonian

The effective spin $S = \frac{1}{2}$, Ising formalism is appropriate for the interaction Hamiltonian. This may be seen from the form of the crystal-field levels of the Tb^{3+} ions.² The lowest levels are a pair of closely spaced singlets (separation⁸ $\delta \approx 1.3$ K), and only these levels are thermally populated at temperatures below about 30 K, the ex-

cited levels being very much higher in energy (> 150 K). The lowest levels form an effective spin $S = \frac{1}{2}$ pair with an exceedingly anisotropic magnetic response. The principal values of the g tensor^{1,2,8} are $g^{zz} = 17.8$, $g^{xx} = g^{yy} = 0$. The crystal may only be magnetized along the c axis, therefore, apart from a Van Vleck susceptibility due to the excited crystal-field levels, and the Van Vleck susceptibility, according to bulk susceptibility data,¹ is negligibly small [$\chi_T^{xx}(\vec{Q} = 0) < 0.01 \chi_T^{zz}(\vec{Q} = 0)$ for $T < 20$ K]. Thus the Ising approximation is very good indeed.

The crystal structure⁹⁻¹¹ for LiTbF_4 is the same as for the mineral scheelite, or CaWO_4 . The space group is $I4_1/a$, and the body-centered unit cell contains four formula units. The Tb^{3+} ions are at the positions (Fig. 1),

$$\begin{aligned} \vec{r}_1 &= (0, 0, \frac{1}{2}c_0), \\ \vec{r}_2 &= (0, \frac{1}{2}a_0, \frac{3}{4}c_0), \\ \vec{r}_3 &= (\frac{1}{2}a_0, \frac{1}{2}a_0, 0), \\ \vec{r}_4 &= (\frac{1}{2}a_0, 0, \frac{1}{4}c_0). \end{aligned} \quad (3)$$

Positions 3 and 4 are obtained from 1 and 2 by the body-centering translation ($a_0/2, a_0/2, c_0/2$). In the primitive unit cell, which has a volume of half the tetragonal unit cell, only sites 1 and 2 need be included. LiTbF_4 is therefore a two-sublattice magnet. However, the Tb^{3+} sites are all magnetically equivalent, with point symmetry S_4 , in the absence of an applied field.

The Hamiltonian must describe the interactions of a given effective spin $S_{\vec{r}_i, \vec{\tau}_i}$ at the i th position

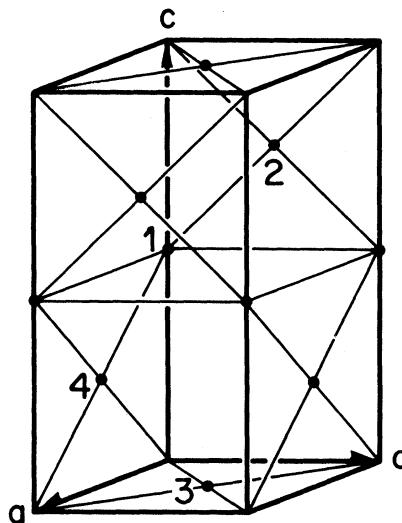


FIG. 1. Tb^{3+} positions in the body-centered tetragonal unit cell of LiTbF_4 .

in the l th unit cell with all other spins in the lattice. Including an applied magnetic field $H^z(\vec{r})$ along the z axis, the Hamiltonian takes the form

$$\begin{aligned} \mathcal{H} = & - \sum_{i,i'} \sum_{m,j} S_{\vec{R}_i, \vec{r}_i}^z K^{zz}(\vec{R}_i + \vec{r}_i - \vec{R}_m - \vec{r}_j) S_{\vec{R}_m, \vec{r}_j}^z \\ & + g^{zz} \mu_B \sum_{i,i'} H^z(\vec{R}_i + \vec{r}_i) S_{\vec{R}_i, \vec{r}_i}^z + \delta \sum_{i,i'} S_{\vec{R}_i, \vec{r}_i}^\perp. \end{aligned} \quad (4)$$

The prime on the summation sign means "omit the term for which the argument of K^{zz} vanishes." We include nondipolar (presumably superexchange) interactions (J^{zz}) and dipolar interactions (D^{zz}) in the potential,

$$\begin{aligned} K^{zz}(\vec{R}_i + \vec{r}_i - \vec{R}_m - \vec{r}_j) = & J^{zz}(\vec{R}_i + \vec{r}_i - \vec{R}_m - \vec{r}_j) \\ & + D^{zz}(\vec{R}_i + \vec{r}_i - \vec{R}_m - \vec{r}_j), \end{aligned} \quad (5)$$

where

$$D^{zz}(\vec{r}) = \frac{1}{2}(g^{zz} \mu_B)^2 [3(r^z)^2 - |\vec{r}|^2] / |\vec{r}|^5. \quad (6)$$

In the expression for \mathcal{H} the term involving the crystal-field splitting δ is seen to be formally equivalent to an uniform magnetic field applied transverse (\perp) to the spin axis. We shall drop this term in the following, for its effect on the high-temperature susceptibility is negligible. Indeed, its effect on $\chi_T(\vec{Q})$ in the critical region is also expected to be small,¹² although one can make the argument with perhaps less rigor in that temperature range. It is fairly easy to calculate $\chi_T(\vec{Q})$ from Eq. (4) for a system of noninteracting spins ($K^{zz} = 0$). The result for $\delta = 0$ is a simple Curie law,

$$\chi_T^0 = (g^{zz} \mu_B)^2 / 4kT, \quad (7)$$

while the result for $\delta \neq 0$ involves the hyperbolic tangent of $\delta/2kT$. Holding $g^{zz} = \text{const.}$, the ratio of the susceptibility for $\delta \neq 0$ to that for $\delta = 0$ is given by the expression

$$(2kT/\delta) \tanh(\delta/2kT). \quad (8)$$

Thus, the finite splitting δ decreases χ_T^0 from Eq. (7) by an amount which increases from zero at high temperatures to, e.g., 8% at $T = \delta/k$, which would be 1.3 K in LiTbF_4 . Above $T = 10$ K, the corrections to χ_T^0 due to $\delta \neq 0$ are less than 1% in LiTbF_4 , and therefore are quite negligible compared to the effects of the interactions among the Tb^{3+} ions.

B. $\chi_T(\vec{Q})$ at high temperatures

An expression for $\chi_T(\vec{Q})$ may be obtained from the Hamiltonian in Eq. (4) with the help of mean-

field theory, which gives a high-temperature approximation to the susceptibility. Neglecting the terms in δ as discussed above, the mean-field equations take the form¹³

$$\begin{aligned} \mu(\vec{R}_i + \vec{r}_i) = & \chi_T^0 \left(H^z(\vec{R}_i + \vec{r}_i) + \frac{2}{(g^{zz} \mu_B)^2} \right. \\ & \left. \times \sum_{m,j} K^{zz}(\vec{R}_i + \vec{r}_i - \vec{R}_m - \vec{r}_j) \mu(\vec{R}_m + \vec{r}_j) \right) \end{aligned} \quad (9)$$

where $\mu(\vec{R}_i + \vec{r}_i)$ is the net magnetic moment in the applied field on the Tb^{3+} ion at position $\vec{R}_i + \vec{r}_i$, and χ_T^0 is the susceptibility per ion of the noninteracting system, as given in Eq. (7), and where $H^z(\vec{R}_i + \vec{r}_i)$ may be taken from Eq. (1), with $\vec{H}(0) \parallel [001]$. As there are two ions in the unit cell of LiTbF_4 (i or $j = 1, 2$), there are therefore $2N$ coupled equations to solve, where N is the number of unit cells.

The Fourier-transform technique facilitates the solution of the equations. We first pass over to a continuous representation in real space, replacing formally the system of magnetic point dipoles at the Tb^{3+} sites by a spatially varying moment density or magnetization function, $M(\vec{r})$. For a given site, the moment density may be defined with the help of the Dirac δ function $\Delta(\vec{r})$ as

$$M_{ii}(\vec{r}) = \mu(\vec{R}_i + \vec{r}_i) \Delta(\vec{r} - \vec{R}_i - \vec{r}_i), \quad (10a)$$

so that

$$\mu(\vec{R}_i + \vec{r}_i) = \int d^3r M_{ii}(\vec{r}). \quad (10b)$$

Note that the units of $M_{ii}(\vec{r})$ are those of magnetization (magnetic moment/volume). The magnetization function describing the distribution of magnetic moments on sublattice i is

$$M_i(\vec{r}) = \sum_j M_{ij}(\vec{r}), \quad (10c)$$

and for the crystal as a whole,

$$M(\vec{r}) = \sum_i M_i(\vec{r}). \quad (10d)$$

The Fourier transform of $M(\vec{r})$ is

$$M_{\vec{Q}} = V^{-1} \int d^3r e^{-i\vec{Q} \cdot \vec{r}} M(\vec{r}), \quad (11)$$

where V is the (large) volume of the crystal (equal to N times the volume of the primitive unit cell). Using Eqs. (10), we find

$$M_{\vec{Q}} = \sum_i M_{i, \vec{Q}}, \quad (12)$$

where

$$M_{i,\vec{Q}} = V^{-1} \sum_i e^{-i\vec{Q}\cdot(\vec{R}_i+\vec{r}_i)} \mu(\vec{R}_i+\vec{r}_i). \quad (13)$$

From Eq. (9),

$$M_{i,\vec{Q}} = \chi_T^0 \left(V^{-1} \sum_i e^{-i\vec{Q}\cdot(\vec{R}_i+\vec{r}_i)} H^z(\vec{R}_i+\vec{r}_i) + \frac{2V^{-1}}{(g^{zz}\mu_B)^2} \sum_{i,m,j} e^{-i\vec{Q}\cdot(\vec{R}_i+\vec{r}_i)} \times K^{zz}(\vec{R}_i+\vec{r}_i-\vec{R}_m-\vec{r}_j) \mu(\vec{R}_i+\vec{r}_i) \right). \quad (14)$$

The first term inside the large parentheses in Eq. (14) is found using Eq. (1) to be N/V times the Fourier transform $H_{\vec{Q}}$ of the applied magnetic field:

$$H_{\vec{Q}} = V^{-1} \int d^3r e^{-i\vec{Q}\cdot\vec{r}} H^z(\vec{r}). \quad (15)$$

The second term in the large parentheses may be simplified by applying the constraints of lattice periodicity. Introducing generalized Curie-Weiss temperatures

$$\Theta_{ij}(\vec{Q}) = (1/2k) \sum_i' e^{-i\vec{Q}\cdot(\vec{R}_i+\vec{r}_i-\vec{r}_j)} K^{zz}(\vec{R}_i+\vec{r}_i-\vec{r}_j) \quad (16)$$

in Eq. (14), we find

$$M_{i,\vec{Q}} = (N/V) \chi_T^0 H_{\vec{Q}} + \sum_j [\Theta_{ij}(\vec{Q})/T] M_{j,\vec{Q}}. \quad (17)$$

Thus the $2N$ -coupled equations have been reduced to only two in Eq. (17). These may easily be solved for $M_{1,\vec{Q}}$ and $M_{2,\vec{Q}}$, and the susceptibility evaluated from Eqs. (2) and (12). The result, expressed on a per ion basis, is

$$\chi_T^0/\chi_T(\vec{Q}) = 1 - \text{Re}[\Theta_{11}(\vec{Q}) + \Theta_{21}(\vec{Q})]/T - \{\text{Im}[\Theta_{21}(\vec{Q})]/T\}^2 / \{1 + \text{Re}[\Theta_{21}(\vec{Q}) - \Theta_{11}(\vec{Q})]/T\}. \quad (18)$$

Note that $\Theta_{ij}(\vec{Q})$ in Eq. (18) may in general be complex. This is because the Tb³⁺ ions are not situated on the centers of inversion in the crystal lattice. However, the ions on a given sublattice i form a Bravais lattice, and $\Theta_{ii}(\vec{Q})$ is therefore real. One can also show that

$$\Theta_{11}(\vec{Q}) = \Theta_{22}(\vec{Q}). \quad (19)$$

A center of inversion is situated midway between sites 1 and 2 and on the line connecting the two sites. It follows that $\Theta_{12}(\vec{Q})$ and $\Theta_{21}(\vec{Q})$ are complex conjugates of one another,

$$\Theta_{12}(\vec{Q}) = \Theta_{21}^*(\vec{Q}). \quad (20)$$

Thus two parameters, the real quantity $\Theta_{11}(\vec{Q})$ and the complex quantity $\Theta_{12}(\vec{Q})$, govern the wave vector dependence of the susceptibility at a given temperature. These parameters are essentially Fourier transforms of respectively the intra- and intersublattice interactions in the crystal.

At long wavelengths ($|\vec{Q}|\approx 0$), the imaginary part of $\Theta_{21}(\vec{Q})$ is negligibly small,

$$\{\text{Im}[\Theta_{21}(\vec{Q})]\}_{|\vec{Q}|\approx 0} \sim Q^z [(Q^x)^2 - (Q^y)^2]. \quad (21)$$

Under these conditions Eq. (18) reduces to the simpler form,

$$\chi_T^0/\chi_T(\vec{Q}) = 1 - \Theta(\vec{Q})/T, \quad (22)$$

with

$$\Theta(\vec{Q}) = \text{Re}[\Theta_{11}(\vec{Q}) + \Theta_{21}(\vec{Q})]. \quad (23)$$

Even for finite \vec{Q} , Eq. (18) reduces to Eq. (22) at high temperatures (where, in fact, the mean-field approximation is "good"), and also for wave vectors along certain high-symmetry directions, e.g., parallel or transverse to the spin axis.

C. Dipolar calculations

The dipolar contributions to $\Theta_{ij}(\vec{Q})$ in LiTbF₄ may be evaluated using Ewald's technique.¹⁴ In this technique the slowly converging series in Eq. (16) is converted into two other series which converge more rapidly than the original. One of these is evaluated in the direct lattice, the other in the reciprocal lattice. Ewald's technique facilitates the carrying out of a long-wavelength expansion^{15, 16} appropriate to Eq. (22) and allows for rapid numerical evaluation of $\Theta_{ij}^{\text{dip}}(\vec{Q})$ for arbitrary wave vectors.

It is convenient to introduce a new set of parameters $A_{ij}^{zz}(\vec{Q})$, which are related to the dipolar part of $\Theta_{ij}(\vec{Q})$ as follows:

$$\Theta_{ij}^{\text{dip}}(\vec{Q}) = -\chi_T^0 T A_{ij}^{zz}(-\vec{Q}). \quad (24)$$

These new parameters are chosen to be analogous to the tensor quantity $A^{\alpha\beta}(\vec{Q})$ of Ref. 16. Our parameters are a generalization of $A^{zz}(\vec{Q})$ to the situation in which there is more than one atom in the unit cell, and, in fact, $A_{ij}^{zz}(\vec{Q}) = A^{zz}(\vec{Q})$ if $i=j$. The analytical definition of $A_{ij}^{zz}(\vec{Q})$, by analogy with Ref. 16, is as follows:

$$A_{ij}^{zz}(\vec{Q}) = \lim_{\vec{r} \rightarrow 0} A_{ij}^{zz}(\vec{Q}, \vec{r}), \quad (25)$$

where

$$A_{ij}^{zz}(\vec{Q}, \vec{r}) = -\frac{\partial^2}{\partial z^2} \sum_i' \frac{e^{i\vec{Q}\cdot(\vec{R}_i+\vec{r}_i-\vec{r}_j)}}{|\vec{R}_i+\vec{r}_i-\vec{r}_j-\vec{r}|}. \quad (26)$$

The prime on the summation means "omit the term with $\vec{R}_i+\vec{r}_i-\vec{r}_j=0$." The quantities $A_{ij}^{zz}(\vec{Q})$

are seen to be independent of the size of the magnetic moments, but dependent on the lattice structure and parameters. The units are those of $(\text{length})^{-3}$.

An additionally useful set of parameters $A_j^{zz}(\vec{Q})$ may be defined as

$$A_j^{zz}(\vec{Q}) = \sum_i A_{ij}^{zz}(\vec{Q}). \quad (27)$$

These linear combinations of the $A_{ij}^{zz}(\vec{Q})$ are appropriate to the long-wavelength limit Eq. (22) for $\chi_T(\vec{Q})$. The parameters $A_j^{zz}(\vec{Q})$ in LiTbF_4 are independent of j near $\vec{Q}=0$, and are related to $\Theta(\vec{Q})$ in Eq. (23) as follows:

$$\Theta(\vec{Q} \approx 0) = -\chi_T^0 \text{Tr}[A_j^{zz}(-\vec{Q})] \delta_{\approx 0}. \quad (28)$$

However, there is another reason for introducing these parameters, and that is because they are useful in checking the dipolar calculations. This may be seen as follows. Suppose we start with a cubic unit cell and put a basis of atoms at, e.g., the origin and face centers. Then the calculated $A_j^{zz}(\vec{Q})$ must be independent of j and equal to the $A^{zz}(\vec{Q})$ of Ref. 16 for a primitive fcc lattice. This point is considered further in Appendix B.

Proceeding now with the calculations, we start from Eq. (26) and apply Ewald's technique to express $A_{ij}^{zz}(\vec{Q})$ in a more rapidly convergent form. The resulting expression is rather complicated and is given in Appendix A, Eqs. (A1)–(A9). A singularity of the form $(Q^z/|\vec{Q}|)^2$ is apparent from the $h=0$ term of Eq. (A2). Using Eqs. (27) and (28) together with the results in Appendix A, we find that near $\vec{Q}=0$ in LiTbF_4 , $\Theta^{\text{dip}}(\vec{Q})$ may be written as follows:

$$\Theta^{\text{dip}}(\vec{Q} \approx 0) = -C_1(Q^z/|\vec{Q}|)^2 + C_2(Q^z)^2 + C_3 + C_4|\vec{Q}|^2 + O((Q^x)^4, (Q^y)^4, \dots). \quad (29)$$

The constants C_1 to C_4 may themselves be expressed as Ewald series and have been evaluated in LiTbF_4 with the help of a computer. Taking

$$g^{zz} = 17.8 \pm 0.1 \quad (30)$$

from Ref. 1, and, for the lattice parameters,

$$a_0 = 5.181(3) \text{ \AA}, \quad (31)$$

$$c_0 = 10.873(6) \text{ \AA},$$

from a crystallographic study at $T=100$ K (following paper), we find

$$C_1 = 8.50 \pm 0.10 \text{ K},$$

$$C_2 = 11.81 \pm 0.13 \text{ K \AA}^2, \quad (32)$$

$$C_3 = 3.97 \pm 0.04 \text{ K},$$

$$C_4 = -5.40 \pm 0.06 \text{ K \AA}^2.$$

These results are somewhat altered from the constants A_1 to A_4 quoted in an earlier publication,^{3, 17} which were based on older values for the lattice parameters. The uncertainties are due mostly to the uncertainty in g^{zz} . The uncertainties in the lattice parameters are small, and the lattice parameters are expected to remain relatively constant at temperatures below 100 K.

Extending our considerations to finite wave vectors, we start now from the equations for $A_{ij}^{zz}(\vec{Q})$ in Appendix A. A computer program based on these equations was written to evaluate $A_{ij}^{zz}(\vec{Q})$ for arbitrary wave vectors in LiTbF_4 . The quantities $\Theta_{ij}^{\text{dip}}(\vec{Q})$ were then evaluated with the help of Eq. (24). The results which are relevant for this paper are given in Fig. 2. Here we consider wave vectors \vec{Q} along the spin axis $\vec{Q}=(0, 0, Q_0)$ or perpendicular to it $\vec{Q}=(Q_0, 0, 0)$. For these limiting cases (which are the ones investigated experimentally in LiTbF_4), the general expression Eq. (18) for $\chi_T(\vec{Q})$ reduces to the simpler form in Eq. (22). Thus, in Fig. 2 we plot the dipolar part of $\Theta(\vec{Q})$ as defined in Eq. (23) as a function of wave vector. If \vec{Q} is applied along the z axis, $\Theta^{\text{dip}}(\vec{Q})$ remains always negative, but varies smoothly between -4.5 K (in the long-wavelengths limit $\vec{Q} \rightarrow 0$) and -2.2 K. For \vec{Q} applied transverse to the z axis, Θ^{dip} varies from $+4.0$ K (in the long-wavelength limit $\vec{Q} \rightarrow 0$) and -3.1 K [e.g., for \vec{Q} midway between the origin and the (200) reciprocal-lattice point]. The patterns shown in Fig. 2 repeat, of course, indefinitely through the reciprocal lattice.

The long-wavelength singularity in Eq. (29) yields a different value for $\Theta^{\text{dip}}(\vec{Q} \rightarrow 0)$ depending on the direction in which the origin \vec{Q} space is approached.

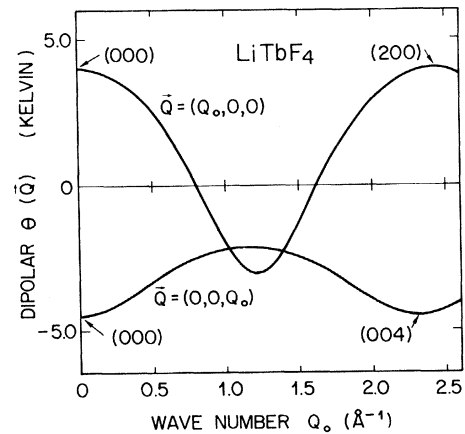


FIG. 2. Calculated dipolar contributions to $\Theta(\vec{Q})$ in LiTbF_4 . The curves shown here repeat indefinitely through the reciprocal lattice. Note that $\Theta(\vec{Q}=0)$ is multiple valued for an infinite crystal.

This is apparent in the curves in Fig. 2. These results obtain for an infinite sample of LiTbF_4 . In a real crystal (e.g., a sphere of diameter L), the results are accurate when \vec{Q} is sufficiently large that many wavelengths of magnetic field are contained within the sample (i.e., for $|\vec{Q}| \gg 2\pi/L$). In the neutron experiment to be described below, $\chi_T(\vec{Q})$ data were obtained for $0.05 \text{ \AA}^{-1} \leq |\vec{Q}| \leq 2 \text{ \AA}^{-1}$. For this range of $|\vec{Q}|$ values, the sample "appeared" infinite, but the minimum $|\vec{Q}|$ was sufficiently small to accurately probe the long-wavelength singularity in $\chi_T(\vec{Q})$ (cf. Fig. 2), and the maximum $|\vec{Q}|$ was sufficiently large to cover a significant part of the $\Theta(\vec{Q})$ curves.

D. Nondipolar interactions

The nondipolar or superexchange part of the interaction potential in Eq. (5) cannot be evaluated analytically, in contrast to the dipolar part, at least not to a high enough degree of accuracy for our purposes. We resort to the usual trick of incorporating unknown "exchange parameters" in the formalism, with the idea of determining these parameters empirically from the data. Fortunately, the parameters so determined turn out to be small compared to the dipolar coupling in LiTbF_4 .

Superexchange coupling has its origins in electrostatic energies associated with the overlapping of single-ion electronic wave functions.¹⁸ The coupling path is presumably from Tb^{3+} to Tb^{3+} via F^- orbitals, and the coupling is expected to fall off rapidly with increasing distance between Tb^{3+} ions. In LiTbF_4 , each Tb^{3+} ion is at the center of a nearest-neighbor (nn) shell containing four Tb^{3+} ions (shell radius 3.75 \AA), a next-nearest-neighbor (nnn) shell containing four Tb^{3+} ions (shell radius 5.18 \AA), a third-neighbor shell containing eight Tb^{3+} ions (shell radius 6.40 \AA), etc. We shall allow for nn and nnn exchange parameters only, which we identify by the notation J_1 and J_2 , respectively. Combining Eqs. (5) and (16) and considering the known crystal structure, we find, for the exchange contributions to $\Theta_i(\vec{Q})$, the following expressions:

$$\begin{aligned} \text{Re}[\Theta_{12}^{\text{ex}}(\vec{Q})] &= (\frac{1}{2}\Theta_{\text{nn}}^{\text{ex}} \cos(\frac{1}{4}c_0 Q^2) [\cos(\frac{1}{2}a_0 Q^x) \\ &\quad + \cos(\frac{1}{2}a_0 Q^y)]), \\ \text{Im}[\Theta_{12}^{\text{ex}}(\vec{Q})] &= (\frac{1}{2}\Theta_{\text{nn}}^{\text{ex}} \sin(\frac{1}{4}c_0 Q^2) [\cos(\frac{1}{2}a_0 Q^x) \\ &\quad - \cos(\frac{1}{2}a_0 Q^y)]), \\ \text{Re}[\Theta_{11}^{\text{ex}}(\vec{Q})] &= (\frac{1}{2}\Theta_{\text{nnn}}^{\text{ex}}) [\cos(a_0 Q^x) + \cos(a_0 Q^y)], \\ \text{Im}[\Theta_{11}^{\text{ex}}(\vec{Q})] &= 0, \end{aligned} \quad (33)$$

where

$$\begin{aligned} \Theta_{\text{nn}}^{\text{ex}} &= 2J_1/k, \\ \Theta_{\text{nnn}}^{\text{ex}} &= 2J_2/k. \end{aligned} \quad (34)$$

Thus, $\Theta_{\text{nn}}^{\text{ex}}$ is the amount by which the paramagnetic Curie temperature $\Theta(\vec{Q}=0)$ is increased due to nn superexchange coupling, and $\Theta_{\text{nnn}}^{\text{ex}}$ is the corresponding quantity for nnn superexchange coupling. We may expand Eqs. (33) about $\vec{Q}=0$ to find, considering the definition Eq. (23),

$$\begin{aligned} \Theta^{\text{ex}}(\vec{Q} \approx 0) &= (\Theta_{\text{nn}}^{\text{ex}} + \Theta_{\text{nnn}}^{\text{ex}}) - (\frac{1}{64}c_0^2) \Theta_{\text{nn}}^{\text{ex}}(Q^x)^2 \\ &\quad - (\frac{1}{16}a_0^2) (\Theta_{\text{nn}}^{\text{ex}} + \Theta_{\text{nnn}}^{\text{ex}}) [(Q^x)^2 + (Q^y)^2] + \dots \end{aligned} \quad (35)$$

The total $\Theta(\vec{Q} \approx 0)$ is given of course by the sum of Eqs. (29) and (35). Comparing the two equations, one can easily show that unless the condition

$$(J_1 + 4J_2)/k > -1.6 \text{ K} \quad (36)$$

is fulfilled, the peak in $\Theta(\vec{Q})$ will move away from $\vec{Q}=0$ into the Brillouin zone, in qualitative disagreement with the experimental findings.

III. EXPERIMENT

Crystals of LiTbF_4 were grown from the melt using a modified Stockbarger technique.¹⁹ The material appears colorless and optically transparent. For the neutron measurements a single crystal was ground to a sphere of 7-mm diameter and mounted in a helium cryostat for control of the temperature down to 1.2 K. In previous experiments we had noticed a tendency for the crystals to flake apart in regions of inhomogeneous strain, e.g., at the interface between sample and glue in a conventional mounting arrangement. To eliminate this problem the sample was held in the present experiments by means of two spring-loaded, bowl-shaped, aluminum caps.

This paper is concerned with the quasielastic neutron scattering from LiTbF_4 over a range of \vec{Q} values at a single temperature $T=18.6 \text{ K}$. The data were taken in a three-axis spectrometer on the Danish Reactor DR-3 at Risø. No inelasticity in the scattering was detected, to within the resolution width of 0.1 meV, in selected initial scans at various wave vectors and temperatures. The resolution of the analyzer was relaxed to 3 meV in carrying out the actual data scans at $T=18.6 \text{ K}$, and the spectrometer was set for elastic scattering. This arrangement discriminated against transitions to the higher crystal-field levels (at energies $> 13 \text{ meV}$) and resulted in a relatively low background count rate. Neutrons of energy 41 meV were selected by the graphite monochromator for the experiment, this energy being close to the peak in the flux distribution obtainable from the reactor.

Under the conditions described above, the quasielastic approximation to the scattering cross section is applicable. For magnetic scattering from

LiTbF₄ this takes the form¹³

$$\sigma(\vec{Q}) = \alpha[1 - (Q^z/|\vec{Q}|)^2]f^2(|\vec{Q}|)\chi_T(\vec{Q})/\chi_T^0, \quad (37)$$

where \vec{Q} is the wave vector transfer

$$\vec{Q} = \vec{k}_1 - \vec{k}_2 \quad (38)$$

of neutrons scattered from wave vector \vec{k}_1 to \vec{k}_2 . The Tb³⁺ magnetic form factor $f(|\vec{Q}|)$ in Eq. (37) is known to high accuracy from recent studies²⁰ of the ferromagnetic compound Tb(OH)₃. Thus, apart from the over-all scaling factor α , which is independent of \vec{Q} and T , the scattered intensity provides a direct measure of the susceptibility ratio $\chi_T(\vec{Q})/\chi_T^0$ for comparison with theory in, e.g., Eq. (18).

The geometrical factor $[1 - (Q^z/|\vec{Q}|)^2]$ in Eq. (37) has its origins in the form of the magnetic interactions between the neutrons and the magnetic moments in the crystal. No magnetic scattering is present for wave vectors along the spin axis in an Ising magnet. Scans with $\vec{Q} \parallel [001]$ in LiTbF₄ therefore provide a means of estimating the nonmagnetic background count rate.

Defining the deviation of \vec{Q} from reciprocal-lattice vector $\vec{\tau}_{200}$ by

$$\vec{q} = \vec{Q} - \vec{\tau}_{200}, \quad (39)$$

we note from the constraints of crystal symmetry that

$$\chi_T(\vec{Q} + \vec{\tau}_{200}) = \chi_T(\vec{q}). \quad (40)$$

The geometrical factor $[1 - (Q^z/|\vec{Q}|)^2]$ in Eq. (37) is nonvanishing for $\vec{q} \parallel [001]$, and so measurements around $\vec{\tau}_{200}$ were used to study $\chi_T(\vec{q})$ for \vec{q} parallel as well as transverse to the spin axis.

IV. RESULTS AND ANALYSIS

In Fig. 3 the results of two large- \vec{q} scans at $T = 18.6$ K are presented. At this temperature the data are considerably more sensitive to the interactions among the Tb³⁺ ions than were the preliminary measurements in Ref. 3 at $T = 38.8$ K. The nuclear peaks (e.g., at $\vec{\tau}_{200}$ and $\vec{\tau}_{202}$) would be far off scale in Fig. 3 and have been omitted from the diagram. Also omitted are a few selected points [e.g., near $\vec{q} = (0.3, 0, 0)\text{\AA}^{-1}$], at positions where the count rate was anomalously high, due to $\frac{1}{2}\lambda$, $\frac{1}{3}\lambda$, . . . , contamination of the incident beam as well as multiple Bragg reflections. We are left, nevertheless, with some 80 data points which may be used in determining the form and magnitude of the interactions in the material.

The three sets of curves in Fig. 3 represent successively higher-order approximations to the scattering cross section. The nonmagnetic background count rate was taken to be $C_B = 400$, this

value having been determined from a separate scan with \vec{Q} along the z axis. The curves in Fig. 3 were least-squares fitted to the data. Fit No. 1 shows the results of neglecting the interactions among the Tb³⁺ ions. The susceptibility ratio in Eq. (37) was set equal to unity, and only the scale factor was optimized to $\alpha = 2375$. The information about magnetic interactions is contained essentially in the difference counts between fit No. 1 and the data. In the next approximation (fit No. 2) dipolar interactions, as described in Sec. IIC, were included in the expression for $\chi_T(\vec{Q})$. Again, α was optimized, this fit giving $\alpha = 2420$. The dipolar-only approximation is quite good, a fact which had been noted previously³ based on less precise data. Nevertheless, the difference in counts between the minimum and maximum of the upper set of data is overestimated by fit No. 2, and this leaves room for improvement by including non-dipolar interactions.

In the third approximation, near-neighbor "exchange" interactions were included in the expression for $\chi_T(\vec{Q})$. Three parameters, the scale factor α and two exchange parameters, J_1 and J_2 (cf. Sec. IID), were allowed to vary freely. The resulting fit No. 3 is seen to be improved over the dipolar-only approximation. The derived values for the parameters are $\alpha = 2440 \pm 15$ and

$$\begin{aligned} J_1/k &= -0.26 \pm 0.09 \text{ K}, \\ J_2/k &= +0.05 \pm 0.10 \text{ K}, \end{aligned} \quad (41)$$

where the state uncertainties are derived from projections of the standard deviation ellipsoid on the appropriate parameter axes. In the fitting procedure the data were weighted according to the Poisson uncertainty of the corresponding intensities. Changing the weighting factors to unity did not shift J_1 and J_2 beyond the stated uncertainties, and the fit was equally insensitive to $\pm 10\%$ changes in the value used for C_B .

V. DISCUSSION

The derived J_1 and J_2 may be compared with other estimates of the nondipolar interactions in LiTbF₄. The temperature dependence of the susceptibility provides, through the Curie-Weiss temperature, a measure of the algebraic sum of the interactions in the material. Defining

$$\Theta^0 = \lim_{q_0 \rightarrow 0} [\Theta(\vec{q})]_{\vec{q} = (q_0, 0, 0)}, \quad (42)$$

we find, from Eqs. (16), (23), and (29),

$$\Theta^0 = C_3 + \Theta_{\text{tot}}^{\text{ex},0}, \quad (43)$$

where $\Theta_{\text{tot}}^{\text{ex},0}$ is the total nondipolar contribution to Θ^0 ,

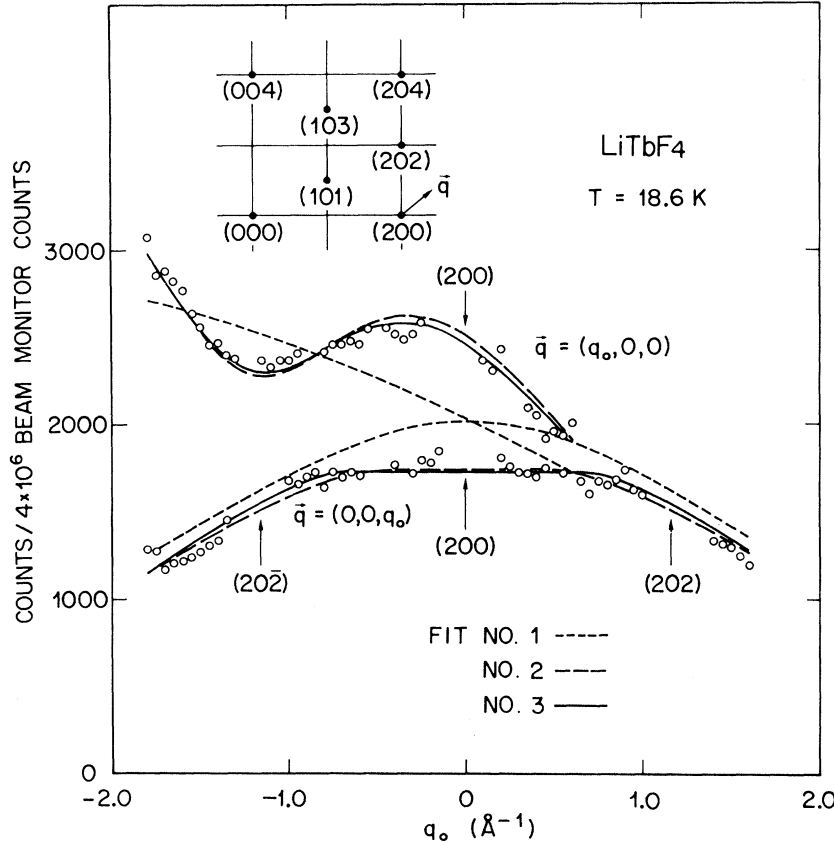


FIG. 3. Quasielastic neutron scattering from LiTbF₄ at $T/T_C = 6.5$. Inset shows a section of the reciprocal lattice defining the deviation wave vector \vec{q} . Nuclear Bragg peaks (at the arrows) have been omitted. Fit Nos. 1, 2, and 3 include, respectively, (1) no interactions among the Tb³⁺ ions, (2) magnetic dipolar coupling only, and (3) magnetic dipolar coupling plus exchange coupling.

$$\Theta_{\text{tot}}^{\text{ex},0} = \frac{1}{2k} \sum_{m,j} J(\vec{R}_m + \vec{r}_j - \vec{r}_i). \quad (44)$$

In the model used for fit No. 3,

$$\Theta_{\text{tot}}^{\text{ex},0} = 2(J_1 + J_2)/k. \quad (45)$$

Experimentally, Θ^0 was determined from neutron scattering data ($\Theta^0 = 3.72 \pm 0.20$ K) in Ref. 3, and from bulk magnetic susceptibility data ($\Theta^0 = 3.60 \pm 0.10$ K) in Ref. 1. Combining these numbers with the calculated dipolar constant C_3 in Eqs. (32), we obtain

$$\Theta_{\text{tot}}^{\text{ex},0} = -0.25 \pm 0.20 \text{ K} \quad (46)$$

from the neutron data and

$$\Theta_{\text{tot}}^{\text{ex},0} = -0.37 \pm 0.11 \text{ K} \quad (47)$$

from the susceptibility data. From Eqs. (41) and (45) we find

$$\Theta_{\text{tot}}^{\text{ex},0} = -0.42 \pm 0.13 \text{ K} \quad (48)$$

from the present results, to be compared with Eqs. (46) and (47).

The relatively low accuracy in the numbers quoted in Eqs. (41) and in Eqs. (46)–(48) is a manifestation of the fact that the nondipolar inter-

actions are simply not very important in LiTbF₄. This is true for $\Theta_{\text{tot}}^{\text{ex},0}$, which is only 10% of C_3 , and it is true as well for the individual exchange parameters. Let the dipolar coupling of a pair of nn spins [cf. Eq. (6)] be D_1 , and let D_2 be the corresponding quantity for nnn spins. Direct calculation yields

$$\begin{aligned} D_1/k &= +1.07 \pm 0.01 \text{ K}, \\ D_2/k &= -0.71 \pm 0.01 \text{ K}. \end{aligned} \quad (49)$$

Comparing with Eqs. (41), we find, for the ratios of exchange to dipolar parameters

$$\begin{aligned} J_1/D_1 &= -0.24 \pm 0.10, \\ J_2/D_2 &= -0.07 \pm 0.15. \end{aligned} \quad (50)$$

Thus, the exchange coupling is only ~25% of the corresponding dipolar interaction for nn Tb³⁺ ions, and it is smaller for second neighbors.

VI. CONCLUSIONS

This paper has presented new information relating to the form and magnitude of the magnetic interactions in LiTbF₄. The mean-field approximation to the wave-vector-dependent susceptibility

$\chi_T(\vec{Q})$ has been derived and the dipolar interactions have been evaluated numerically. Singlet-singlet effects for the non-Kramers ion Tb^{3+} have been considered and shown to be unimportant at high temperatures (> 10 K). Experimental neutron scattering data have been obtained at $T = 18.6$ K and analyzed in terms of the theoretical expression for $\chi_T(\vec{Q})$, including, in addition to the dipolar coupling, two "exchange" parameters J_1 and J_2 . The exchange parameters have been evaluated empirically [Eqs. (41)] and found to be considerably smaller than even the nearest-neighbor dipolar coupling alone [Eqs. (50)]. Our earlier conclusion that LiTbF_4 forms a model system for the study of magnetic dipolar interactions has therefore been reinforced and made quantitative in this work.

ACKNOWLEDGMENT

We are grateful to Professor G. Busch for his interest and encouragement in this project.

APPENDIX A: EWALD'S METHOD IN LiTbF_4

The analytical procedure used in applying Ewald's technique to evaluating dipolar summations has been amply described elsewhere,¹⁴ and will not be reviewed in detail. Here we present for reference purposes, and in outline form only, the results for LiTbF_4 .

As described in Appendix A of Ref. 16, and in Ref. 14, the quantities $A_{ij}^{zz}(\vec{Q})$ may be converted from Eqs. (25) and (26) into the following form:

$$A_{ij}^{zz}(\vec{Q}) = \alpha_{ij}^{zz}(\vec{Q}) + \beta_{ij}^{zz}(\vec{Q}) + \gamma_{ij}^{zz}(\vec{Q}), \quad (\text{A1})$$

in which the quantities on the right-hand side are defined in terms of summations over the direct and reciprocal lattices. The first term, $\alpha_{ij}^{zz}(\vec{Q})$, is a summation over all reciprocal lattice vectors²¹ \vec{Q}_h ,

$$\alpha_{ij}^{zz}(\vec{Q}) = \frac{1}{v_A} \sum_h G_3 \left(\frac{R}{|\vec{Q} + \vec{Q}_h|} \right) \frac{(Q^z + Q_h^z)^2}{|\vec{Q} + \vec{Q}_h|^2} e^{-i\vec{Q}_h \cdot \vec{r}_{ij}}, \quad (\text{A2})$$

where v_A is the volume of the unit cell in the direct lattice, R is the "Ewald parameter" to be chosen for rapid convergence of the series (see below), and \vec{r}_{ij} is a vector connecting sites i and j in the unit cell:

$$\vec{r}_{ij} = \vec{r}_i - \vec{r}_j. \quad (\text{A3})$$

For arbitrary ξ ,

$$G_3(\xi) = 4\pi e^{-(1/4\xi^2)}. \quad (\text{A4})$$

The quantity $\beta_{ij}^{zz}(\vec{Q})$ is a sum over all nonzero vectors in the direct lattice,

$$\beta_{ij}^{zz}(\vec{Q}) = - \sum_{\vec{r} \neq 0} H_{zz}^{3,R}(\vec{R}_i + \vec{r}_{ij}) e^{+i\vec{Q} \cdot (\vec{R}_i + \vec{r}_{ij})}, \quad (\text{A5})$$

where

$$H_{zz}^{3,R}(\vec{R}_i + \vec{r}_{ij}) = R \lim_{\vec{r} \rightarrow 0} \frac{\partial^2}{\partial z^2} H(R|\vec{R}_i + \vec{r}_{ij} - \vec{r}|), \quad (\text{A6})$$

and, for general ξ ,

$$H(\xi) = \frac{2}{\xi\sqrt{\pi}} \int_{\xi}^{\infty} dy e^{-y^2}. \quad (\text{A7})$$

The remaining term in Eq. (A1), $\gamma_{ij}^{zz}(\vec{Q})$, is evaluated differently for $\vec{r}_{ij} = 0$ and $\vec{r}_{ij} \neq 0$. For $\vec{r}_{ij} \neq 0$, $\gamma_{ij}^{zz}(\vec{Q})$ has the same form as $\beta_{ij}^{zz}(\vec{Q})$, but with $\vec{R}_i = 0$,

$$\gamma_{ij}^{zz}(\vec{Q}) = -H_{zz}^{3,R}(\vec{r}_{ij}) e^{i\vec{Q} \cdot \vec{r}_{ij}} \text{ if } \vec{r}_{ij} \neq 0. \quad (\text{A8})$$

For $\vec{r}_{ij} = 0$, $\gamma_{ij}^{zz}(\vec{Q})$ reduces to a real constant,

$$\left. \begin{aligned} \text{Re} \gamma_{ij}^{zz}(\vec{Q}) &= -(4R^3/3\sqrt{\pi}) \\ \text{Im} \gamma_{ij}^{zz}(\vec{Q}) &= 0 \end{aligned} \right\} \text{ if } \vec{r}_{ij} = 0. \quad (\text{A9})$$

For large \vec{R}_i and \vec{Q}_h ,

$$H_{zz}^{3,R}(\vec{R}_i) \sim e^{-R^2|\vec{R}_i|^2}, \quad (\text{A10})$$

whereas

$$G_3(R/|\vec{Q}_h|) \sim e^{-|\vec{Q}_h|^2/4R^2}. \quad (\text{A11})$$

The expression (A1) is independent of R , but, from (A10) and (A11) it is seen that Eqs. (A2) and (A5) converge more rapidly for R small and large, respectively. In practice R is chosen as a compromise to ensure reasonably fast convergence of both summations.

The expressions (A1) to (A9) are generally valid and not restricted to the special structure of LiTbF_4 . Implicit in the formulation, however, is the assumption that the z component of the \underline{g} tensor is the same for all ions in the unit cell.

APPENDIX B. CHECKING THE CALCULATIONS—CUBIC LATTICES

An expression for $A_j(\vec{Q})$, analogous to Eq. (29) for $\Theta(\vec{Q})$, may be obtained from the equations in Appendix A in the long-wavelength ($\vec{Q} \approx 0$) limit,

$$A_j^{zz} = a_1(Q^z/|\vec{Q}|)^2 - (a_2 - a_5)(Q^z)^2 - a_3 - a_4(|\vec{Q}|)^2 + O(Q^z[(Q^x)^2 - (Q^y)^2], (Q^z)^4, \dots). \quad (\text{B1})$$

The notation here in terms of the constants a_i , $i = 1, 2, \dots, 5$, parallels that of Ref. 16. The coefficients a_1 , $(a_2 - a_5)$, etc., are real and independent of j in LiTbF_4 . The inequivalence of the two Tb^{3+} sites shows up first in terms of order $Q^z[(Q^x)^2 - (Q^y)^2]$. Comparing with Eqs. (28) and (29), we see that

TABLE I. Coefficients in the long-wavelength expression for $A_j^{zz}(\vec{Q})$ in cubic lattices.

Lattice symmetry	sc			bcc	fcc
	Case 1	Case 2	Case 3		
Unit cell parameters					
a_0	1	1	2	$2/\sqrt{3}$	$\sqrt{2}$
b_0	1	1	2	$2/\sqrt{3}$	$\sqrt{2}$
c_0	1	2	2	$2/\sqrt{3}$	$\sqrt{2}$
Atoms unit cell	1	2	8	2	4
Coordinates of basis atoms	(0, 0, 0)	(0, 0, 0) (0, 0, $\frac{1}{2}$)	(0, 0, 0) ($\frac{1}{2}$, 0, 0) (0, $\frac{1}{2}$, 0) (0, 0, $\frac{1}{2}$) ($\frac{1}{2}$, $\frac{1}{2}$, 0) (0, $\frac{1}{2}$, $\frac{1}{2}$) ($\frac{1}{2}$, 0, $\frac{1}{2}$) ($\frac{1}{2}$, $\frac{1}{2}$, $\frac{1}{2}$)	(0, 0, $\frac{1}{2}$) ($\frac{1}{2}$, $\frac{1}{2}$, 0)	(0, 0, 0) (0, $\frac{1}{2}$, $\frac{1}{2}$) ($\frac{1}{2}$, 0, $\frac{1}{2}$) ($\frac{1}{2}$, $\frac{1}{2}$, 0)
a_1	12.5664	12.5664	12.5664	16.3242	17.7715
$a_2 - a_5$	-0.4945	-0.4945	-0.4945	0.9644	1.0058
a_3	4.1888	4.1888	4.1888	5.4414	5.9238
a_4	0.1648	0.1648	0.1648	-0.3215	-0.3353

$$C_i = \chi_T^0 T a_i, \quad i = 1, 3, 4, \quad (\text{B2})$$

$$C_2 = \chi_T^0 T (a_2 - a_5).$$

After the computer program for calculating the constants C_i in LiTbF₄ was written, it was a simple matter to distort the unit cell so as to generate lattices of simple cubic (sc), body-centered-cubic (bcc), and face-centered-cubic (fcc) symmetries. The constants, a_1 , $(a_2 - a_5)$, etc., could then be evaluated for comparison with Table I of Ref. 16 and with Ref. 15. The calculated values are given in Table I. Note that the nearest-neighbor distance is unity for each of the lattices considered.

For a given cubic lattice the coefficients a_i are theoretically constrained by the relations¹⁶

$$a_5 - a_2 = 3a_4 \quad (\text{B3})$$

and

$$a_1 = 3a_3. \quad (\text{B4})$$

Each of the four constants in Table I was evaluated

separately for each lattice, and the resulting values are seen to satisfy Eqs. (B3) and (B4) very accurately.

The computer program was written in such a way that the unit cell could be tetragonal and could include more than one atomic site. These two aspects of the program were tested for lattices of over-all sc symmetry, as shown in columns 2 and 3 of Table I. The calculations gave the same results for each of the three sc cases shown, and these results agree with those in Table I of Ref. 16.

The numerical results for the fcc and bcc lattices in Table I are in disagreement with those quoted in Table I of Ref. 16, but this discrepancy has been traced to a misprint in Eq. (18) of Ref. 15, from which source Table I of Ref. 16 was in part prepared.²² Thus the results in Table I are correct and confirm the validity of the computational technique.

*Work partly performed while on leave from Bell Laboratories as a guest scientist at AEC Research Establishment, Risø, Denmark. Research at ETH, Zürich supported by the Schweizerischer Nationalfonds zur Förderung der Wissenschaftlichen Forschung.

¹L. M. Holmes, T. Johansson, and H. J. Guggenheim *Solid State Commun.* **12**, 993 (1973).

²L. M. Holmes, H. J. Guggenheim, and J. Als-Nielsen, in *Proceedings of the International Conference on Magnetism* (Nauka, Moscow, 1974), Vol. VI, p. 256.

³J. Als-Nielsen, L. M. Holmes, and H. J. Guggenheim, *Phys. Rev. Lett.* **32**, 610 (1974).

⁴J. Als-Nielsen, L. M. Holmes, F. Krebs Larsen, and H. J. Guggenheim, following paper, *Phys. Rev. B* **12**, 191 (1975).

⁵J. Als-Nielsen, L. M. Holmes, and J. J. Guggenheim (unpublished).

⁶See, e.g., R. M. White, *Quantum Theory of Magnetism* (McGraw-Hill, New York, 1970).

⁷The implications of this statement are discussed by

- W. P. Wolf and co-workers in connection with "high-temperature" specific-heat and susceptibility measurements on the rare-earth (*R*) hydroxides $R(\text{OH})_3$; A. T. Skjeltorp, C. A. Catanese, H. E. Meissner, and W. P. Wolf, *Phys. Rev. B* **7**, 2062 (1973); C. A. Catanese, A. T. Skjeltorp, H. E. Meissner, and W. P. Wolf, *ibid.* **8**, 4223 (1973).
- ⁸The neutron study in Ref. 2 gave $\delta < 2$ K. A recent EPR investigation of Tb-substituted LiYF_4 gave $\delta = 1.34$ K. I. Laursen and L. M. Holmes, *J. Phys. C* **7**, 3765 (1974).
- ⁹R. E. Thoma, C. F. Weaver, H. A. Friedman, H. Insley, L. A. Harris, and H. A. Yakel, Jr., *J. Phys. Chem.* **65**, 1096 (1961).
- ¹⁰C. Keller and H. Schmutz, *J. Inorg. Nucl. Chem.* **27**, 900 (1965).
- ¹¹R. E. Thoma, C. D. Brunton, R. A. Penneman, and T. K. Keenan, *Inorg. Chem.* **9**, 1096 (1970).
- ¹²R. J. Elliott, P. Pfeuty, and C. Wood, *Phys. Rev. Lett.* **25**, 443 (1970).
- ¹³cf. W. Marshall and S. W. Lovesey, *Theory of Thermal Neutron Scattering* (Clarendon, Oxford, 1971), Chap. 13.
- ¹⁴See, e.g., M. Born and K. Huang, *Dynamical Theory of Crystal Lattices* (Oxford U. P., Oxford, 1954), Sec. 30.
- ¹⁵M. H. Cohen and F. Keffer, *Phys. Rev.* **99**, 1128 (1955); *Phys. Rev. B* **10**, 787(E) (1974).
- ¹⁶A. Aharony and M. E. Fisher, *Phys. Rev. B* **8**, 3323 (1973).
- ¹⁷The numerical value of A_4 should have been negative ($A_4 = -5.392 \text{ K \AA}^2$) rather than positive as given under Eq. (4) in Ref. 3.
- ¹⁸P. W. Anderson, in *Magnetism*, edited by G. T. Rado and H. Suhl (Academic, New York, 1963), Vol. I, p. 25.
- ¹⁹H. J. Guggenheim, *J. Appl. Phys.* **34**, 2482 (1963).
- ²⁰G. H. Lander, T. O. Brun, J. P. Desclaux, and A. J. Freeman, *Phys. Rev. B* **8**, 3237 (1973).
- ²¹The notation \vec{Q}_h is used for simplicity in writing out the rather complicated equations in Appendix A. $\vec{\tau}_{hkl}$ is used in the text.
- ²²This was confirmed in a private communication from F. Keffer (cf. Ref. 15, Erratum). We should also like to acknowledge correspondence with A. Aharony on this point.